*I.J. Image, Graphics and Signal Processing,* **2026, 3, 1-16**
Published Online on June 8, 2026 by MECS Press (http://www.mecs-press.org/)
DOI: 10.5815/ijigsp.2026.03.01

# A Feature-Enhanced Hybrid CNN-BiLSTM Framework for Multi-Label Classification of Pathological High-Frequency Oscillations in Intracranial EEG Signals

**Rahma Maalej***
University of Sfax, Miracl Lab, Department of STIC, National School of Electronics and Telecommunications of Sfax, Tunisia
E-mail: rahmamaalej1234@gmail.com
ORCID iD: https://orcid.org/0009-0006-7040-9698
*Corresponding author

**Abir Hadriche**
University of Sfax, Research Groups in Intelligent Machines, Regim Lab, Digital Research Center of Sfax, CRNS, Enis, High institute of Music, Sfax, Tunisia
E-mail: Abir.hadriche.tn@ieee.org
ORCID iD: https://orcid.org/0000-0002-2908-0230

**Mohamed Amine Ben Msarra**
University of Sfax, Miracl Lab, Department of STIC, National School of Electronics and Telecommunications of Sfax, Tunisia
E-mail: medaminebenmsarra@gmail.com
ORCID iD: https://orcid.org/0009-0005-5946-0129

**Nawel Jmail**
University of Sfax, Miracl Lab, Digital Research Center of Sfax, CRNS, Higher Business School, Sfax, Tunisia
E-mail: naweljmail@yahoo.fr
ORCID iD: https://orcid.org/0000-0003-0823-9641

Received: January 5, 2026; Revised: February 19, 2026; Accepted: March 10, 2026; Published: June 8, 2026

**Abstract:** Interictal high-frequency oscillations, including ripples in the frequency range of 80-250 hertz and fast ripples between 250-500 hertz, are increasingly recognized as reliable electrophysiological biomarkers for delineating the epileptogenic zone in patients with drug-resistant epilepsy. However, their routine clinical exploitation remains limited due to pronounced morphological variability, low signal-to-noise ratios, and the difficulty of identifying overlapping events in which ripples and fast ripples occur simultaneously.

This paper presents an automated deep learning framework designed for the multi-label classification of pathological high-frequency oscillations in intracranial electroencephalographic signals. The proposed approach integrates advanced nonlinear statistical descriptors, including entropy- and complexity-based measures, in order to enhance the discriminative representation of the signals. These features are processed using a hybrid deep learning architecture that combines convolutional neural networks for local morphological feature extraction with bidirectional long short-term memory networks to capture long-range temporal dependencies in non-stationary neural signals.

The proposed framework was evaluated using the publicly available multi-patient intracranial electroencephalography dataset provided by the Collaborative Research in Computational Neuroscience initiative. Experimental results demonstrate a classification accuracy of 98.3 %, along with high precision and balanced performance across all pathological classes. These findings indicate that the proposed method offers a robust and objective solution for the automated identification of high-frequency oscillations, with strong potential for improving presurgical evaluation and decision-making in epilepsy surgery.

**Index Terms:** High-Frequency Oscillations, Intracranial Electroencephalography, Multi-Label Classification, Hybrid Deep Learning Architecture, Nonlinear Signal Analysis, Epileptogenic Zone Localization

This work is open access and licensed under the Creative Commons CC BY 4.0 License.

## 1. Introduction

Epilepsy remains one of the most prevalent and complex neurological disorders, affecting approximately 1% of the global population and exceeding 50 million people worldwide [1]. Despite the continuous expansion of the pharmacological arsenal, approximately one-third of patients develop drug-resistant epilepsy, where seizures persist despite optimal medical treatment. For these individuals, surgical resection of the epileptogenic zone (EZ) often represents the only viable path toward seizure freedom. However, the success of such surgical interventions relies heavily on the precision with which pathological neural networks are delineated. This challenge is particularly acute in cases of bilateral temporal lobe epilepsy, where identifying drug-resistant laterality is critical for surgical planning [2]. In this framework, intracranial electroencephalography (IEEG) has emerged as the gold-standard diagnostic tool, offering unparalleled spatio-temporal resolution for exploring epileptic foci [3].

Over the past decade, High-frequency Oscillations (HFOs) categorized into Ripples (80–250 Hz) and Fast Ripples (250–500 Hz) have been identified as paramount electrophysiological biomarkers for localizing the EZ [4]. Unlike classical interictal spikes, Fast Ripples are more closely linked to the brain tissue capable of generating seizures. Recent advancements in SEEG analysis have shown that combining high-frequency energy with synchronous connection analysis in epileptic networks significantly enhances EZ localization [5]. Furthermore, the integration of multi-epileptogenic biomarker machine learning has proven effective in automating the detection of these zones in drug-resistant patients [6]. Complementary studies have also investigated source localization and connectivity metrics for oscillatory activities in other modalities like MEG, providing a broader context for electrophysiological signal characterization [7].

Nevertheless, the systematic adoption of HFOs in clinical routine faces major hurdles. Manual identification by experts is a tedious task, prone to significant inter-observer variability, and further complicated by the low signal-to-noise ratio of these transient events. Moreover, HFO morphology varies considerably across patients and can be easily confounded with physiological activities or instrumental artifacts [8]. Effective characterization often requires robust separation between spikes and oscillatory activities, which has been explored through stationary wavelet transforms on embedded architectures [9]. While classical outlier detection methods like "smart" k-nearest neighbor (k-NN) are being developed to catalyze EEG signal analysis [10] and switching state space models are improving HFO detection from raw IEEG data [11], advanced decomposition techniques like consensus matching pursuit have been used to handle signal variability [12]. Nevertheless, there remains a pressing need for more robust, deep-learning-driven solutions. This is especially critical as the field evolves toward comprehensive automated detection and seizure recognition frameworks tailored for the 2022–2025 clinical landscape [13].

To address these challenges, numerous automated systems have been proposed. Recent studies have explored multi-classification approaches using deep learning models on iEEG signals to better categorize complex neural events [14]. However, most existing methods are limited to binary detection (HFO vs. non-HFO), thereby neglecting the complexity of "overlapping" events where Ripples and Fast Ripples occur simultaneously (FRandR events). These hybrid events are clinically significant but difficult to isolate. Furthermore, while Deep Learning, specifically, Convolutional Neural Networks (CNN) has shown promising performance [15], many models treat IEEG signals as static images. Recent trends have shifted toward capturing temporal dynamics using Recurrent Neural Networks (RNN) for seizure detection [16] or employing dual attention mechanisms to prioritize relevant EEG features [17]. To specifically distinguish epileptic HFOs from non-HFO events, recent studies have successfully employed vision-language frameworks, such as the pre-trained OWL-ViT model combined with LSTM layers, which offer a reliable approach for signal characterization [18]. Furthermore, advanced spatiotemporal models are increasingly utilized to enhance the detection and recognition of complex epileptic EEG patterns, providing more robust frameworks for characterizing non-stationary neural signals [19].

To bridge these gaps, this study introduces an advanced hybrid framework specifically engineered for the multi-label classification of HFOs. Our approach synergizes state-of-the-art nonlinear statistical descriptors with a deep architecture that merges CNNs and Bidirectional Long Short-Term Memory (BiLSTM) networks. This dual perspective extracting local morphological features via convolutional layers while simultaneously modeling long-term temporal dependencies through spatiotemporal mechanisms [20] is essential for accurately characterizing the oscillatory nature of HFOs within noisy IEEG environments.

The main contributions of this work are summarized as follows:

- Multi-Label Classification Paradigm: We propose a model capable of simultaneously distinguishing three distinct pathological classes (Ripples, Fast Ripples, and R+FR), providing a more granular diagnostic analysis than conventional binary detectors.
- Feature-Enhanced Hybrid Pipeline: We integrate advanced nonlinear descriptors (such as entropy and signal complexity measures) to enrich the deep learning process, ensuring superior robustness against inter-patient variability.

- Optimized CNN–Bi-LSTM Architecture: We designed a specific hybrid structure where the BiLSTM layers refine the recognition of complex temporal patterns, addressing previous criticisms regarding the simplicity of standard architectures.
- Large-Scale Clinical Validation: The proposed framework was validated on a 20-patient dataset (CRCNS IEEG-1), achieving state-of-the-art accuracy (98.3%) and demonstrating high generalization capabilities, which is crucial for potential integration into clinical workflows.

The remainder of this paper is organized as follows: Section 2 provides a comprehensive review of existing automated HFO detection methods; Section 3 details the proposed methodology; Section 4 provides the experimental results and discussion and Section 5 concludes the paper.

## 2. Related Work

The automated detection of HFOs has undergone a significant paradigm shift, transitioning from elementary energy-based detectors to sophisticated deep learning architectures. Early research predominantly focused on providing interpretable tools through hand-crafted features and classical machine learning. For instance, Adusumilli and Bee (2024) [20] simplified seizure detection by combining k-nearest neighbors (k-NN) with fuzzy inference systems, while Padmakala (2025) [21] utilized Random Forest and Support Vector Machines in rodent models. To further refine these traditional approaches, Chaibi and Kachouri (2025) [18] introduced smart k-NN outlier detection to catalyze EEG signal analysis, while Gu et al. (2024) [11] employed switching state space models to specifically isolate HFOs from complex IEEG data. While these techniques offer high interpretability, they inherently struggle with the non-stationary nature and morphological diversity of neural signals, lacking the capacity to learn hierarchical features directly from raw data.

To better capture the intricate morphology of these biomarkers, researchers have increasingly turned toward CNNs for superior spatial feature extraction. Yi et al. (2025) [15] enhanced feature mapping using weighted visibility graphs, and Krikid et al. (2024) [22] focused on improving classification accuracy through targeted data augmentation. Furthermore, Huang et al. (2025) [17] recently proposed a dual-attention mechanism to prioritize relevant spatiotemporal features in EEG recognition. Despite these advancements, CNN-centric models often treat HFOs as static patterns, thereby ignoring the critical temporal context and global dependencies of the signal.

Table 1. Performance and Structural Comparison of State-of-the-Art Epileptic Biomarker Classifiers.

| References | Core Methodology | Key Strengths | Technological Constraints |
|---|---|---|---|
| [5] | High-Frequency Network Analysis | Precise EZ localization via synchronous connectivity. | High sensitivity to electrode placement and coverage. |
| [6] | Multi-Biomarker Machine Learning | Holistic EZ detection via multi-epileptogenic biomarkers. | Requires simultaneous recording of multiple signal types. |
| [10] | Smart k-NN Outlier Detection | Optimized outlier identification for EEG signal cleaning. | Limited by the Euclidean distance metric in high dimensions. |
| [11] | Switching State Space Model | Captures non-linear transitions between HFO and background. | High mathematical complexity for real-time SEEG stream. |
| [15] | Weighted Visibility Graphs | Superior transformation of 1D signals into 2D spatial maps. | Substantial computational latency during graph mapping. |
| [16] | Recurrent Neural Networks | Robust modeling of long-range seizure dependencies. | Vulnerable to gradient vanishing in very high-frequency IEEG. |
| [17] | Dual Attention Mechanism | Focuses on critical spatiotemporal features in epileptic EEG. | Significant memory overhead for attention weight storage. |
| [18] | LSTM + OWL-ViT Framework | Reliable distinction of HFOs using vision-language models. | Dependence on high-quality pre-trained weights for HFOs. |
| [19] | Multi-attention Spatiotemporal | Excellent noise robustness in complex IEEG environments. | Architectural depth requires massive labeled datasets. |
| [20] | KNN-ANFIS Fusion | Robust rule-based decision making for seizure events. | High sensitivity to outliers in raw signal data. |
| [21] | Ensemble Learning (RF/SVM) | Low risk of overfitting on limited clinical samples. | Static feature extraction fails to adapt to signal dynamics. |
| [22] | Augmented CNN | Enhanced model stability via synthetic feature expansion. | Risk of introducing non-physiological artifacts. |
| [23] | Spatio-Temporal CNN–Bi-LSTM | Dual-path processing for extracting complex neural patterns. | Extensive training time due to recurrent layer depth. |
| [24] | Bidirectional Residual LSTM | Efficient gradient flow in long-term temporal sequences. | Significant hyperparameter sensitivity for convergence. |

In response to these challenges, recent studies have emphasized the importance of hybrid spatio-temporal modeling. Kumari et al. (2025) [23] and Zhao et al. (2024) [24] demonstrated that combining CNNs with Bidirectional Long Short-Term Memory (BiLSTM) networks allows for the capture of full signal context. This evolution toward recurrent structures is supported by the work of Aslan and Bingöl (2024) [16], who utilized RNN-based models for robust seizure

classification. To specifically address the HFO vs. non-HFO distinction, Chaibi and Kachouri (2025) [18] integrated LSTM layers with a pre-trained OWL-ViT vision–language framework, achieving high reliability. Additionally, Su et al. (2025) [19] introduced multi-attention mechanisms within spatiotemporal models to enhance recognition accuracy in noisy environments.

At the cutting edge of research, the field is being redefined by the integration of multi-biomarker strategies and advanced multi-branch neural architectures. For instance, Du et al. (2025) [6] utilized multi-epileptogenic biomarker machine learning to automate the detection of the EZ.

These sophisticated methodologies are critical for surgical success, particularly when identifying drug-resistant laterality in complex clinical cases [2]. Nevertheless, the simultaneous multi-label classification of Ripples, Fast Ripples, and overlapping FRandR events persists as a major challenge. Our proposed framework bridges this gap by synergizing nonlinear statistical descriptors with a robust CNN–Bi-LSTM architecture, delivering a more granular and clinically applicable diagnostic tool.

## 3. Proposed Methodology

The architectural framework of the proposed system is systematically organized into an end-to-end automated pipeline, as illustrated in Fig. 1. The process initiates with data acquisition, involving high-resolution IEEG recordings from patients diagnosed with drug-resistant epilepsy. These raw signals undergo a rigorous preprocessing phase, employing a zero-phase Finite Impulse Response (FIR) band-pass filter (80–500 Hz) to isolate pathological HFO frequency bands while strictly preventing phase distortion, followed by meticulous artifact removal to ensure signal integrity. Subsequently, a specialized feature extraction stage is executed to compute a multidimensional set of handcrafted statistical and nonlinear descriptors; these descriptors are specifically engineered to quantify the underlying complexity and chaotic dynamics of the neural oscillations, providing a robust information base that purely data-driven architectures often overlook. To ensure clinical reliability and mitigate overfitting, a strict data allocation protocol partitions the dataset into independent training, validation, and test sets using a patient-independent validation strategy. Finally, the classification stage leverages these features to train and evaluate a proposed hybrid CNN–Bi-LSTM architecture. This model is uniquely engineered to synergize spatial feature learning via convolutional layers with bidirectional temporal dependency modeling through Bi-LSTM units, thereby enabling the precise multi-label distinction between ripples, fast ripples, and the simultaneous occurrence of both events (FRandR) across diverse and non-stationary neural environments.

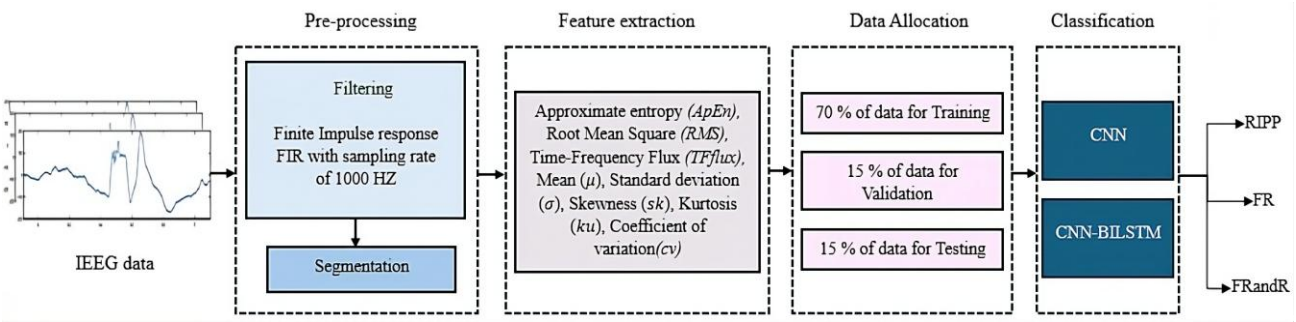


Fig. 1. Detailed workflow of the proposed multi-label HFO classification framework.

### *3.1. Data Description*

In this study, we utilized IEEG recordings from the publicly available CRCNS HFO dataset (IEEG-1) [25]. This corpus comprises long-term invasive recordings from 20 adult patients with drug-resistant focal epilepsy who underwent presurgical evaluation. All data consist of real interictal IEEG signals; no synthetic or simulated data were employed. Ground truth labels are based on expert-validated HFO annotations provided by the CRCNS consortium. The clinical characteristics of the dataset are summarized in Table 2., including age ranges, sex distribution, epilepsy types, electrode configurations, and the volume of annotated data.

The recordings were captured using a combination of subdural strips, grids, and stereotactic depth electrodes, tailored to the clinical requirements of each patient. To minimize interference, 5-minute intervals were selected exclusively from interictal slow-wave sleep, ensuring a minimum three-hour buffer from any seizure event and the absence of stimulation artifacts. Signals were sampled at 2000 Hz and initially provided as monopolar channels referenced to a common intracranial contact.

Table 2. Summary of patient characteristics in the CRCNS IEEG-1 dataset.

| Patients | Age Range | Sex | Epilepsy Type | Electrode Types | Nights | 5-min Intervals |
|---|---|---|---|---|---|---|
| 1–9 | 20–52 | 5M / 4F | Temporal Lobe Epilepsy (TLE) | Depth + Strips | 1–6 | 12–39 |
| 10–20 | 17–49 | 8M / 3F | Extra-Temporal Epilepsy (ETE) | Grids + Depth/Strips | 1–4 | 1–29 |

For each interval, we implemented the validated bipolar montage definition (BipChOrder) provided in the dataset to derive 23 bipolar channels per patient. This bipolar approach was chosen to reduce reference contamination and enhance the spatial specificity of HFO detection. The dataset includes expert annotations for three distinct classes: ripples (RIPP), fast ripples (FR), and combined ripple–fast ripple (FRandR) events. These annotations, following the criteria established by Burnos et al. (2016) [26], specify, the bipolar channel and the precise onset and offset samples, serving as the gold standard for our supervised learning framework. Fig. 2. displays a representative 5-minute annotated interval from patient 1 on first night, illustrating the raw signal alongside the expert-validated HFO markers.

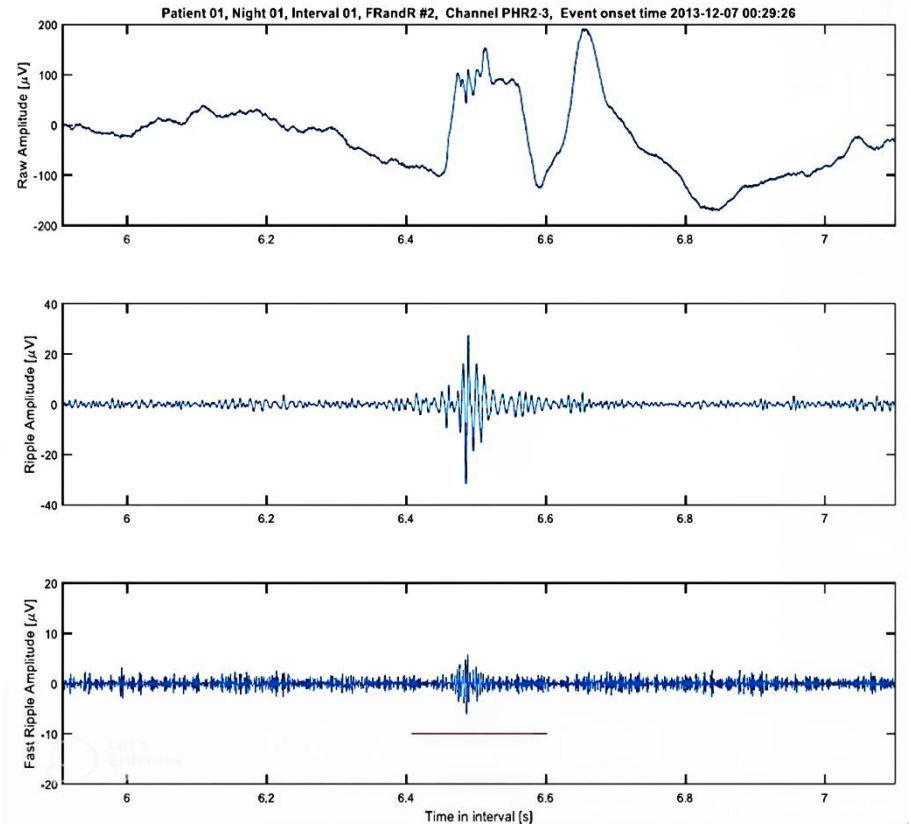


Fig. 2. Overview of patient number 1, night 1 dataset [25].

### *3.2. Data Preprocessing*

Following the CRCNS consortium's recommended protocol, the monopolar contacts were re-referenced into 23 bipolar channels per recording using the provided BipChOrder matrix. Bipolar referencing enhances spatial specificity for localized HFO activity and mitigates the influence of a distant or contaminated reference electrode. For each bipolar derivation $b$, the signal $x_b(t)$ was computed from two adjacent contacts $x_j(t)$ and $x_{j+1}(t)$, as presented in (1):

$$x_b(t) = x_j(t) - x_{j+1}(t) \tag{1}$$

#### *3.2.1. Downsampling and Filtering*

Raw IEEG signals (2000 Hz) were downsampled by a factor of 2 to a working sampling frequency of 1000 Hz, which significantly reduced computational load while preserving the HFO band. The signals were then processed with a zero-phase Finite Impulse Response (FIR) bandpass filter (101 taps), ranging from 80–500 Hz, to isolate ripples and fast ripples. Filtering was applied using the $filtfilt$ function to eliminate phase distortion.

#### *3.2.2. Segmentation*

Each bipolar channel was segmented into non-overlapping windows of 150 samples, corresponding to a duration of 150 ms at 1000 Hz. Each 5-minute interval (300,000 samples) yielded 2,000 segments per channel. The input segment tensor shape prior to the deep learning model was defined by the time samples and the bipolar channels as defined in (2):

$$(150\ samples \times 23\ channels \times 2\ inputs) \tag{2}$$

#### *3.2.3. Label Construction*

The ground-truth labels were derived from the expert-validated annotations for ripples (RIPP), fast ripples (FR), and combined ripple–fast ripple (FRandR) events. These annotations, which specify the channel, onset, and offset, were mapped to the corresponding 150-ms segments. We constructed a multilabel binary label volume, as shown in (3):

$$Y \in \mathbb{R}^{150\times23\times3} \tag{3}$$

where the dimensions represent:

- Time samples: 150
- Channels: 23 bipolar channels
- Classes: 3 (RIPP, FR, FRandR)

Each element $Y[t, c, k]$ is a binary indicator of whether event class $k$ is present at time sample $t$ on channel $c$. Crucially, FRandR events were assigned exclusively to the FRandR class to maintain a non-redundant multilabel target.

#### *3.2.4. Feature Extraction*

Epileptic IEEG signals are characterized by inherent complexity and nonlinearity, making them challenging to analyze using traditional methods. Nonlinear properties of these signals can reveal intricate dynamics and offer more precise, sensitive, and comprehensive insights.

Entropy serves as a critical tool for quantifying these nonlinear features, enabling effective detection and characterization of epileptic events. Approximate entropy quantifies logarithmic conditional probability that a new pattern will occur within a signal sequence as its dimensionality changes. This property makes approximate entropy particularly valuable for characterizing stochasticity and complexity inherent in signal. By preserving time-series information from original signal sequence, approximate entropy reflects structural distribution characteristics of studied data, enhancing its ability to extract meaningful features [27]. Additionally, approximate entropy is highly efficient, requiring fewer data points to provide a statistically robust description of signal sequence [27].

For the computation of approximate entropy, the embedding dimension was set to m = 2 and the tolerance was set to r = 0.2 × SD, where SD is the standard deviation of the segment.

Root Mean Square (RMS) is a time-domain feature commonly used to quantify amplitude magnitude of a signal. It provides a measure of total energy contained in signals over entire period. Calculation process is outlined in (4).

$$RMS = \sqrt{\frac{1}{N}\sum_{i=1}^{N} x_i^2} \tag{4}$$

where x represents the signal amplitude and N denotes the number of samples.

Furthermore, to capture localized spectral energy variations over time in IEEG signals, we extracted Time-Frequency Flux (TFflux) as a feature. TFflux quantifies dynamic redistribution of signal energy across time-frequency domain, reflecting transient patterns that are often indicative of pathological oscillatory activity such as HFOs. This feature has shown potential in characterizing non-stationary signals by measuring changes in spectral energy trajectories across time, which is critical for identifying epileptiform events [27]. Equation (5) presents mathematical formulation of process.

$$TFflux\,[l, r] = \sum_{n=0}^{N-1-l}\ \sum_{m=0}^{M-1-r} |\bar{s}[n+1, m+1] - \bar{s}[n, m] \tag{5}$$

where $\bar{s}[n, m] = |\bar{s}[n, m]|^2$ and $\bar{s}[n, m]$ denotes the time–frequency representation of the intracranial electroencephalographic signal at time index $n$and frequency bin $m$, where $N$and $M$represent the total number of time

samples and frequency bins. In this study, three possible directions are considered for computing time-frequency flux (TFflux):

(i) Along time axis (i.e., l=1, r=0), denoted as $TFflux_1 = TFflux\,[1,0]$;
(ii) Along frequency axis (i.e., l=0, r=1), denoted as $TFflux_1 = TFflux\,[0,1]$;
(iii) Along both time and frequency axes (i.e., l=r=1), denoted as $TFflux_1 = TFflux\,[1,1]$;

In addition to time-frequency flux, we also extracted a set of standard statistical descriptors from time-frequency representations of IEEG and the three directional variants of time-frequency flux (temporal, frequency, and joint time-frequency) were concatenated into a single feature vector to provide a comprehensive representation of spectral dynamics. These include mean μ, standard deviation $\sigma$, skewness $sk$, kurtosis $ku$, and coefficient of variation cv. Traditionally, such features are computed in their time or frequency domain to describe distributional properties of a signal [3]. However, recent studies have demonstrated their relevance when extended to joint time-frequency domain, offering a more localized and dynamic characterization of signal behavior [5]. These features capture not only central tendency and dispersion but also asymmetry and peakedness of spectral energy distribution, making them particularly suitable for detecting transient epileptiform events such as HFOs.

Calculation of standard statistical descriptors is presented in (6) to (11).

$$\mu = \frac{1}{MN}\sum_{n=1}^{N}\sum_{M=1}^{M}\bar{s}\,[n,m] \tag{6}$$

$$\sigma = \sqrt{\frac{1}{MN}\sum_{n=1}^{N}\sum_{M=1}^{M}(\bar{s}[n,m] - \mu)^2} \tag{7}$$

$$sk = \sqrt{\frac{1}{MN\sigma^2}\sum_{n=1}^{N}\sum_{M=1}^{M}(\bar{s}[n,m] - \mu)^3} \tag{8}$$

$$ku = \frac{1}{MN\sigma^4}\sum_{n=1}^{N}\sum_{M=1}^{M}(\bar{s}[n,m] - \mu)^4 \tag{9}$$

$$cv = \frac{\sigma}{\mu} \tag{10}$$

### *3.3. Data Preparation and Splitting*

All 150-ms segments from the 20 patient recordings were aggregated into final data arrays. The aggregated input and label array shapes were defined in (11) and (12):

$$X \in \mathbb{R}^{N\times 150\times 23\times 2} \tag{11}$$

$$Y \in \mathbb{R}^{N\times 150\times 23\times 3} \tag{12}$$

where $N$ is the total number of segments, 150 is the number of time samples, 23 is the number of channels, and 3 is the number of classes.

The dataset was partitioned using a 70% / 15% / 15% patient-stratified split, allocating 14 patients to the training set, 3 patients to the validation set, and 3 patients to the testing set. Crucially, all segments from a single patient were assigned exclusively to one of these subsets. This patient-stratified approach ensures a strictly patient-independent evaluation and prevents any data leakage, as the model is tested on brain activity from individuals it has never encountered during training. This methodology confirms that the performance results reflect the model's ability to generalize to new patients.

### *3.4. Deep Learning Architectures*

#### *3.4.1. Convolutional Neural Network (CNN) Architecture*

The architecture comprises three principal components: convolutional layers (for local feature extraction), pooling layers (for spatial down-sampling and complexity reduction), and fully connected layers (for classification).

The CNN model treats each segment as a 2D input (Time × Channels). Table 3. summarizes the architecture, which utilizes three successive blocks of Conv2D, Batch Normalization (BN), and Max Pooling layers. The final layer uses sigmoid activation to enable multi-label prediction across all output dimensions (150 samples × 23 channels × 3 classes).

The detailed architecture is summarized in Table 3.

Table 3. CNN architecture overview.

| Layer | Parameters | Output shape |
|---|---|---|
| Input | – | 150 × 23 × 1 |
| Conv2D + BN + MaxPool | 32 filters, 3×3, ReLU | 75 × 11 × 32 |
| Conv2D + BN + MaxPool | 64 filters, 3×3, ReLU | 37 × 5 × 64 |
| Conv2D + BN + MaxPool | 128 filters, 3×3, ReLU | 18 × 2 × 128 |
| Flatten | – | 4608 |
| Dense | 256 units, ReLU | 256 |
| Dense | 128 units, ReLU | 128 |
| Dense + Reshape | Sigmoid | 150 × 23 × 3 |

#### *3.4.2. Proposed Hybrid Convolutional Neural Network–Bidirectional Long Short-Term Memory Architecture (CNN–Bi-LSTM)*

To enhance the model's ability to capture temporal dependencies inherent in HFO sequences, we developed a hybrid CNN–Bi-LSTM model. This architecture takes the robust features extracted by the convolutional layers and feeds them into a recurrent layer.

A Long Short-Term Memory (LSTM) network is a specialized type of Recurrent Neural Network (RNN) designed to address the issues of vanishing and exploding gradients over long sequences [29]. The internal architecture of a single LSTM unit is detailed in Fig. 3.

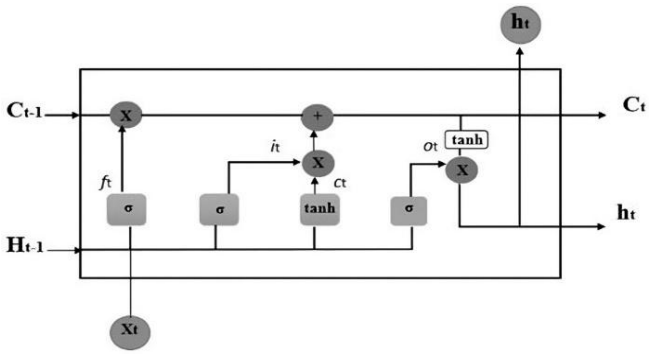


Fig. 3. Architectural schematic of a single LSTM.

The core of the LSTM unit is the cell state, regulated by three mechanisms: the forget gate $f_t$ , the input gate $i_t * \tilde{C}_t$, and the output gate $O_t$. The operations are defined by (13) through (18).

$$f_t = \sigma(W_f . [h_{t-1}, x_t] + b_f \tag{13}$$

$$i_t = \sigma(W_i . [h_{t-1}, x_t] + b_i \tag{14}$$

$$\tilde{C}_t = tanh(W_c . [h_{t-1}, x_t] + b_c \tag{15}$$

$$C_t = f_t * C_{t-1} + i_t * \tilde{C}_t \tag{16}$$

$$O_t = \sigma(W_0 . [h_{t-1}, x_t] + b_0 \tag{17}$$

$$h_t = O_t * tanh(C_t) \tag{18}$$

In (13)–(18), $x_t$represents the input feature vector at time step $t$, $h_{t-1}$and $h_t$denote the previous and current hidden states, and $C_{t-1}$and $C_t$correspond to the previous and current cell states of the long short-term memory unit. The variables $f_t$, $i_t$, and $o_t$denote the forget, input, and output gates, respectively, while $\tilde{C}_t$represents the candidate cell state. The matrices $W_f$, $W_i$, $W_c$, and $W_o$are learnable weight parameters, $b_f$, $b_i$, $b_c$, and $b_o$denote bias terms, and $\sigma(\cdot)$and $\tanh(\cdot)$correspond to the sigmoid and hyperbolic tangent activation functions.

The Bidirectional LSTM (Bi-LSTM) architecture integrates both a forward and a backward LSTM network as illustrated in Fig. 4. This allows the model to access contextual information from both preceding (past) and succeeding (future) states within the 150-ms segment, which is crucial for distinguishing transient pathological HFOs from background activity. In the hybrid model, the final features from the CNN are reshaped and processed by a Bi-LSTM layer (with 0.3 dropout) before the final multilabel output layer.

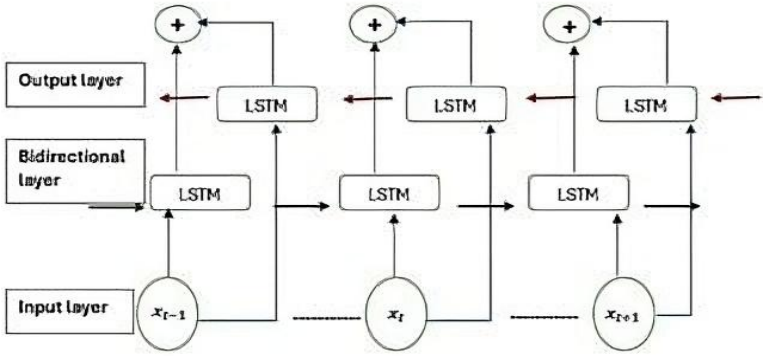


Fig. 4. General architecture of Bi-LSTM recurrent neural network.

### *3.5. Training Parameters*

The handcrafted feature vector (comprising Approximate Entropy, RMS, and Time-Frequency Flux) was integrated into the neural network architecture. These features were fused with the deep spatial-temporal representations by concatenating them immediately after the Flatten layer (in CNN models) or the Bi-LSTM layer (in hybrid models), and prior to the first Dense layer. The final feature vector dimensionality is 15. This fusion strategy ensures that the final classification layer benefits from both the automatically learned deep features and the expert-engineered statistical descriptors before reaching the sigmoid-activated output layer.

Both the baseline CNN and the proposed CNN–Bi-LSTM models were trained with the following parameters:

- Loss Function: Binary Cross-Entropy, suitable for the multi-label classification task.
- Optimizer: Adam (default learning rate 1e-3).
- Batch Size: 512.
- Epochs: 100.
- Regularization: Validation set monitoring was implemented to prevent overfitting.

### *3.6. Performance Evaluation Metrics*

The performance of all models was rigorously evaluated using standard metrics for classification tasks. True Positives ($TP$), False Positives ($FP$), False Negatives ($FN$), and True Negatives ($TN$) were computed at the sample and channel level across all three HFO classes.

- Accuracy: Overall proportion of correctly predicted samples, as presented in (19):

$$Accuracy = \frac{TP + TN}{TP + FN + FP + TN} \tag{19}$$

- Precision: Proportion of true positives among all positive predictions, as defined in (20):

$$Precision = \frac{TP}{TP + FP} \tag{20}$$

- Recall (Sensitivity): Proportion of true positives among all actual positives, expressed in (21):

$$Recall = \frac{TP}{TP + FN} \tag{21}$$

- F1-Score: The harmonic mean of Precision and Recall, providing a balanced measure of performance, detailed in (22):

$$F1 - score = 2 \times \frac{Precision.Recall}{Precision + Recall} \tag{22}$$

## 4. Experimental Evaluation

In In the preceding sections, we developed four distinct classifier families designed to differentiate between three types of HFOs present in iEEG data: ripples (RIPP), fast ripples (FR), and combined ripples with fast ripples (FRandR). These classifiers were implemented using the Python programming language, leveraging the TensorFlow and Keras libraries for deep learning model development.

To ensure a robust and unbiased evaluation, the dataset was partitioned using a patient-stratified split strategy (70% training, 15% validation, and 15% testing). Specifically, out of the 20 patients in the CRCNS dataset, 14 patients were allocated to training, 3 to validation, and 3 to testing. Crucially, all data segments from a single patient were assigned exclusively to one of these subsets. This approach ensures a strictly patient-independent evaluation, preventing data leakage and ensuring that the model is tested on brain activity from individuals it has never encountered during training.

The proposed algorithm leverages extracted features as input to the sigmoid-activated output layer for both CNN and CNN-BiLSTM architectures, enabling effective multi-label classification. During training, we employed the Binary Cross-Entropy (BCE) loss function, which is specifically suited for multi-label tasks where classes are not mutually exclusive. Given that HFO events, particularly Fast Ripples (FR) and FRandR, are naturally rare compared to background activity (RIPP), class distribution was carefully monitored. To ensure the high global accuracy was not biased by the dominant negative class, performance was strictly validated using per-class Precision, Recall, and F1-Score, as reported in Table 4. These balanced metrics remain robust even in the presence of inherent clinical class imbalance.

Fig. 5. illustrates the distribution of classification accuracies (%) for six different deep learning configurations. These include two CNN models with different internal capacities (n64 and n42), the same models enhanced with handcrafted features (+feat), and two hybrid CNN-Bi-LSTM models. It is important to clarify that the labels "n42" and "n64" refer to the architectural configurations (number of convolutional filters and neurons in the hidden layers) rather than the input channel count. All models process the identical 23-channel bipolar input from the dataset.

Overall, all models exhibit high accuracy, typically above 95%. Models incorporating additional features (CNN n64+feat and CNN n42+feat) show more consistent performance, reflected by narrower interquartile ranges (IQRs). The CNN-BiLSTM models demonstrate comparable accuracy but offer better temporal feature extraction. This comparison underscores the robustness of CNN-based models and confirms that augmenting them with expert-engineered features leads to more stable and improved performance across different patient profiles.

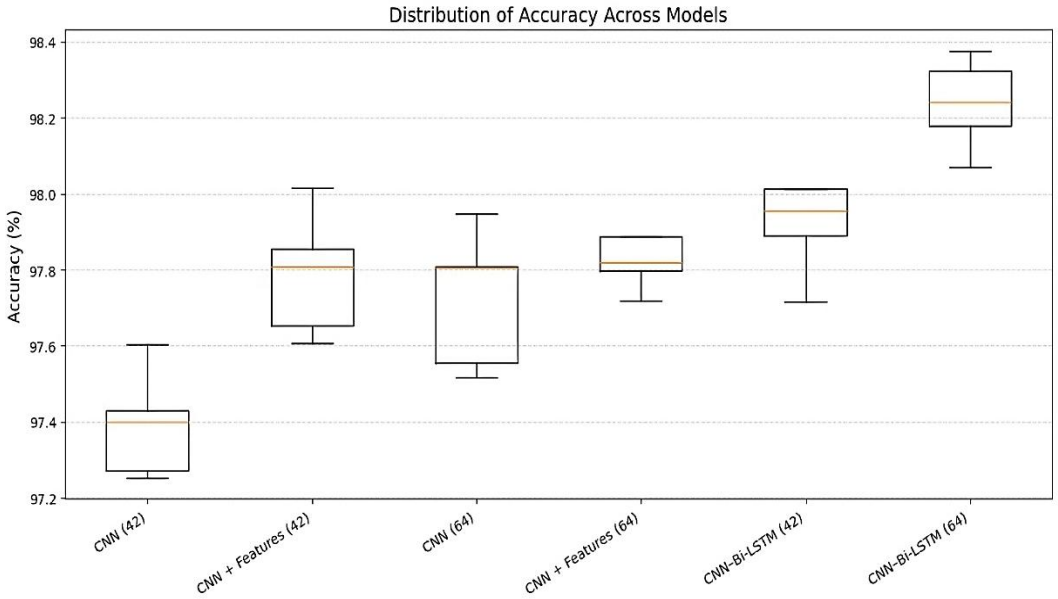


Fig. 5. Distribution of scores for 6 models.

To evaluate the discriminative performance of the proposed classification models, Receiver Operating Characteristic (ROC) curves were plotted, as shown in Fig. 6. The ROC curve illustrates the trade-off between the true positive rate and the false positive rate across different decision thresholds, where a higher area under the curve indicates superior classification performance. Fig. 6(a). and Fig. 6(b). correspond to the convolutional neural network models using sixty-four and forty-two channels, respectively. Fig. 6(c). and Fig. 6(d). present the same architectures augmented with handcrafted features under both channel configurations. Finally, Fig. 6(e). and Fig. 6(f). depict the performance of the hybrid convolutional neural network and bidirectional long short-term memory models using sixty-four and forty-two channels, respectively. The comparative analysis of these curves demonstrates that all models achieve high discriminative capability, with the hybrid architecture exhibiting improved robustness across the three pathological classes.

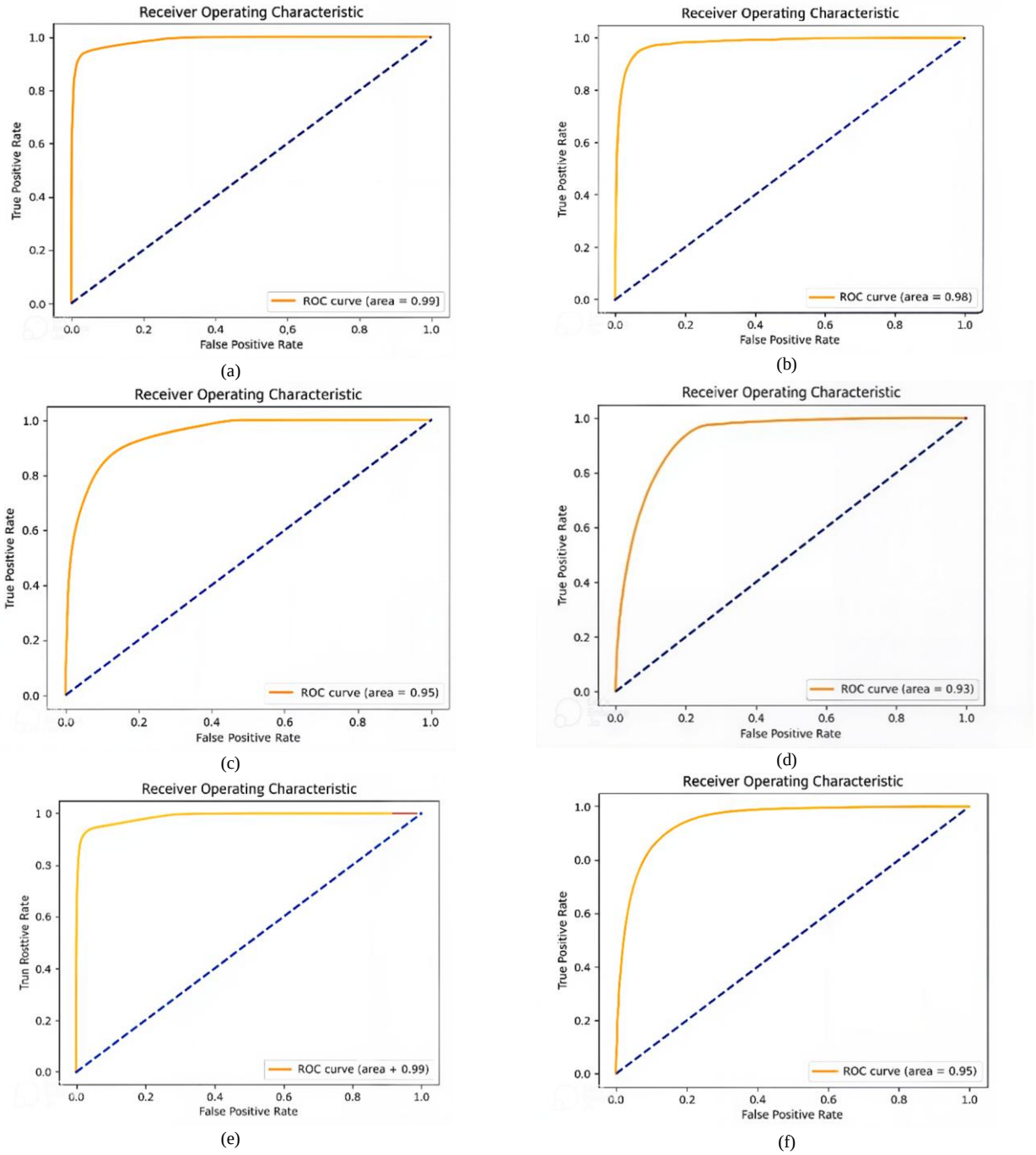


Fig. 6. Receiver operating characteristic curves for the evaluated deep learning models.

To further assess the performance of the proposed models, Precision–Recall curves were generated, as illustrated in Fig. 7. Unlike the Receiver Operating Characteristic curve, which is more suitable for balanced datasets, the Precision–Recall curve provides a more informative evaluation in the presence of class imbalance by emphasizing the trade-off between precision and recall. Fig. 7(a). and fig. 7(b). correspond to the convolutional neural network models using sixty-four and forty-two channels, respectively, while Fig. 7(c). and fig. 7(d). illustrate the same models enhanced with handcrafted features. Fig. 7(e). and fig. 7(f). represent the hybrid convolutional neural network and bidirectional long short-term memory architectures under both channel configurations. The consistently high precision and recall observed across all curves highlight the robustness of the proposed models in detecting seizure-related patterns in intracranial electroencephalographic signals.

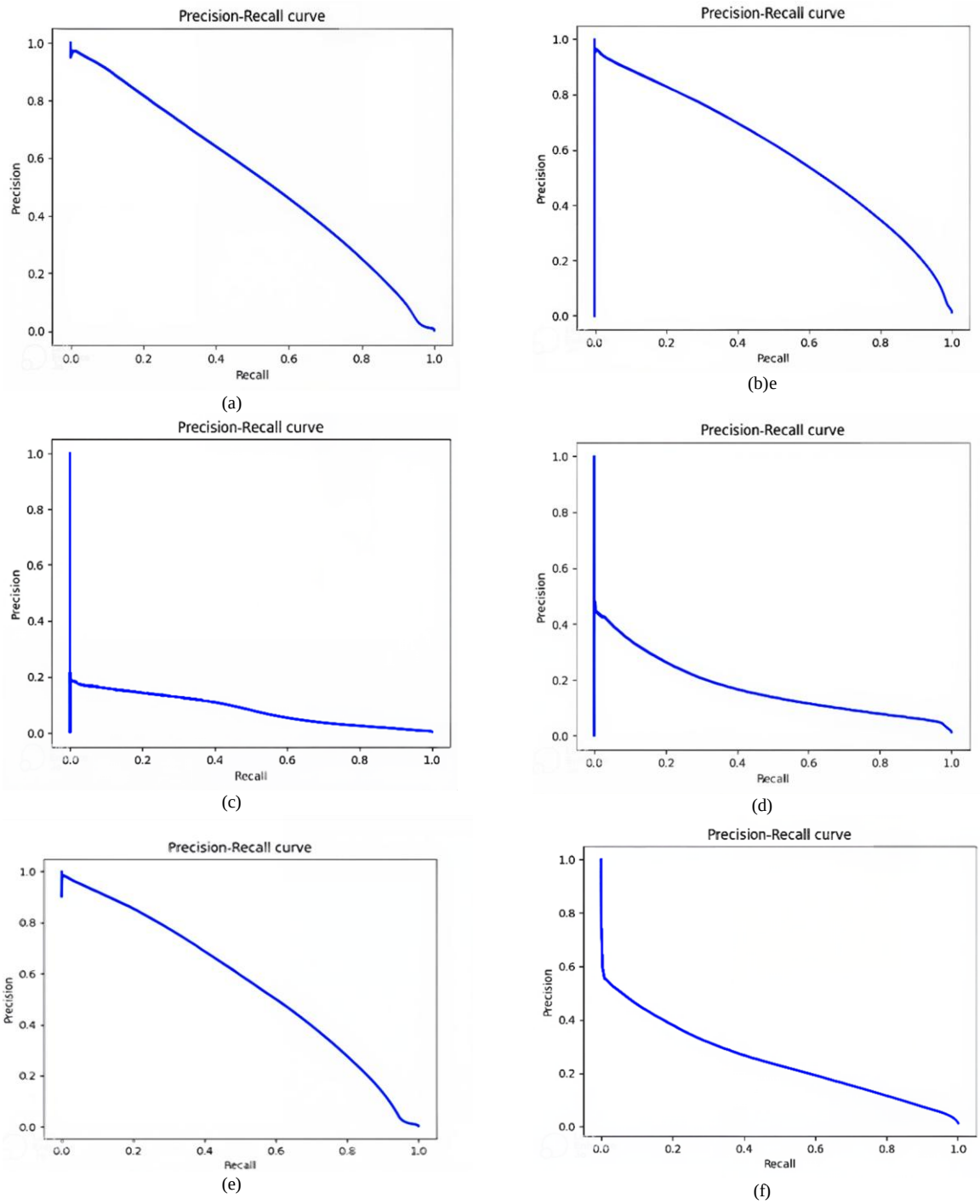


Fig. 7. Precision–Recall curves for the evaluated deep learning models.

Table 4. General performance results of proposed methods on IEEG dataset.

| Model\Metric | Precision (%) | Recall (%) | F1-score (%) | Accuracy (%) |
|---|---|---|---|---|
| CNN (42 channels) | 79.9 | 80.0 | 79.0 | 97.3 |
| CNN + Features (42 channels) | 78.0 | 82.0 | 80.0 | 97.7 |
| CNN (64 channels) | 84.0 | 80.1 | 82.0 | 97.9 |
| CNN + Features (64 channels) | 85.0 | 80.9 | 82.9 | 98.0 |
| CNN–Bi-LSTM (42 channels) | 83.8 | 88.0 | 85.8 | 98.0 |
| CNN–Bi-LSTM (64 channels) | 96.7 | 94.8 | 95.7 | 98.3 |

Table 4. summarizes the classification performance across model configurations and channel settings. The CNN baseline with 42 channels reached 97.3 % accuracy and improved marginally with handcrafted features. The proposed CNN–Bi-LSTM consistently outperformed CNNs, with the best model (64 channels) reaching 98.3 % accuracy, F1 equal to 95.7 %. These results indicate that Bi-LSTM integration enhances temporal modeling and sensitivity to co-occurring/rare HFOs classes, while channel depth and feature augmentation provide modest additional gains.

Table 5. Performance metrics per HFO category for the CNN-Bi-LSTM (n64+feat) model.

| Model | Class | Precision (%) | Recall (%) | F1-Score (%) | Accuracy (%) |
|---|---|---|---|---|---|
| CNN-Bi-LSTM (n64+feat) | Ripples (RIPP) | 98.6 | 94.5 | 96.5 | 98.5 |
| | Fast Ripples (FR) | 97.9 | 91.8 | 94.8 | 98.1 |
| | FRandR | 98.2 | 93.3 | 95.7 | 98.3 |
| | Average (Global) | 98.4 | 93.2 | 95.7 | 98.3 |

A detailed per-class performance analysis is presented in Table 5, providing the Precision, Recall, and F1-score for each HFO category. The results demonstrate that the proposed CNN-Bi-LSTM (n64+feat) model achieves high discriminative power across all classes, including the clinically critical and rare Fast Ripples (FR), which reached an F1-score of 94.8% and a recall of 91.8%. This balanced performance across minority and majority classes confirms that the model does not exploit class imbalance and effectively captures the distinct signatures of various pathological oscillations. The high global average F1-score of 95.7% further validates the robustness of our feature-enhanced hybrid architecture in a multi-label classification context.

This study demonstrates that hybrid deep learning architectures, particularly the proposed CNN–Bi-LSTM model, provide a highly reliable framework for the automated multi-label classification of high-frequency oscillation (HFO) subtypes in drug-resistant epilepsy. The achieved accuracy of 98.3% underscores the effectiveness of synergizing spatial feature extraction with bidirectional temporal modeling, which allows the network to capture the non-stationary evolution of neural signals more effectively than standard convolutional models. A critical factor in this performance is the integration of handcrafted nonlinear statistical descriptors, such as Approximate Entropy and Time-Frequency Flux; these features act as an informed prior, quantifying the chaotic dynamics of the IEEG signal and providing a more stable information base that compensates for the inherent opacity often associated with purely data-driven architectures.

Clinically, our ability to precisely distinguish between ripples, fast ripples, and their simultaneous occurrence (R+FR) is paramount, as the co-localization of these biomarkers is a high-fidelity indicator of the epileptogenic zone's core. By moving beyond traditional spectral thresholds and manual detection rules, this automated framework offers an objective and reproducible tool for presurgical mapping, potentially reducing the subjectivity and time-intensive nature of current clinical workflows. However, certain limitations must be acknowledged, including the focus on an adult-only cohort and the inherent class imbalance between HFO types. Despite these constraints, the high Precision-Recall performance suggests that the model is robust to rare events. Future research should prioritize cross-patient generalizability and the inclusion of pediatric data to ensure that this hybrid framework can be seamlessly integrated into diverse intraoperative environments to improve surgical outcomes and post-operative seizure freedom.

## 5. Conclusion

In this work, we developed and evaluated a robust deep learning framework for the fully automated multi-label classification of HFO subtypes, including ripples, fast ripples, and concurrent ripple–fast ripple (FRandR) events. By comparing a standard CNN architecture with a proposed hybrid CNN–Bi-LSTM model, we demonstrated that while convolutional layers are effective for spatial feature extraction, the integration of bidirectional recurrent modeling is essential for capturing the complex, non-stationary temporal dynamics of pathological HFOs.

The experimental results underscore the superiority of the hybrid approach, which achieved an outstanding accuracy of 98.3% and an F1-score of 95.7% in the 64-channel configuration. These findings highlight that bidirectional temporal context significantly enhances the model's ability to discriminate between subtle morphological patterns and transient artifacts, a critical requirement for clinical reliability. Furthermore, by augmenting the deep learning process with nonlinear statistical descriptors, we have established a reproducible pipeline that bridges the gap between expert-driven signal analysis and automated feature discovery.

Overall, this research advances the development of objective diagnostic tools for presurgical epilepsy evaluation. The proposed framework offers a scalable and precise solution for HFO mapping, potentially improving surgical outcomes for patients with drug-resistant epilepsy. Future work will focus on validation across larger multi-center clinical cohorts to ensure global robustness, as well as investigating event-level localization and the integration of attention mechanisms or Transformer-based architectures [30]. These advancements, building on preliminary hybrid modeling [30], will further refine the interpretability and temporal precision of automated biomarker detection in diverse clinical settings.

## All the Declarations and Statements

### Author Contributions Statement

Rahma Maalej – Conceptualization, Methodology, and Software Implementation: Proposed the hybrid CNN-BiLSTM framework, developed the feature extraction pipeline, and drafted the initial manuscript.
Abir Hadriche – Data Curation and Supervision: Handled the acquisition and preprocessing of the CRCNS IEEG-1 dataset and supervised the experimental design.
Mohamed Amine Ben Msarra – Model Training, Validation, and Performance Evaluation: Executed the model training, performed the patient-stratified cross-validation, and conducted the statistical benchmarking.
Nawel Jmail – Formal Analysis, Writing – Review and Editing, and Project Management: Performed in-depth analysis of the pathological significance of results, reviewed the manuscript for clinical coherence, and coordinated project milestones.

All authors have read and agreed to the published version of the manuscript.

### Conflict of Interest Statement

The authors declare no conflicts of interest.

### Funding Declaration

This research received no specific grant from any funding agency in the public, commercial, or not-for-profit sectors.

### Data Availability Statement

This study analyzed the publicly available CRCNS IEEG-1 dataset. The dataset can be found at: https://crcns.org/datasets/ieeg/ieeg-1, accessed on January 5, 2026.

### Ethical Declarations

The authors declare that this study utilized a publicly available de-identified dataset (CRCNS IEEG-1). Ethical approval was obtained by the original data collectors at the respective clinical institutions, and all procedures involving human subjects were in accordance with the 1964 Helsinki Declaration and its later amendments.

### Acknowledgments

We sincerely thank the anonymous reviewers for their professional evaluation and valuable recommendations, which have significantly contributed to improving the technical clarity and the overall quality of this paper.

#### Declaration of Generative AI in Scholarly Writing

During the preparation of this work, the authors used AI-assisted technologies to improve the linguistic clarity and formatting of the manuscript. After using these tools, the authors reviewed and edited the content as needed and take full responsibility for the content of the published article.

### Abbreviations

The following abbreviations are used in this manuscript:

iEEG - Intracranial Electroencephalography
HFO - High-Frequency Oscillation
RIPP - Ripples
FR - Fast Ripples
FRandR - Fast Ripples and Ripples (overlapping events)
CNN - Convolutional Neural Network
BiLSTM - Bidirectional Long Short-Term Memory
ApEn - Approximate Entropy

RMS - Root Mean Square
TFflux - Time-Frequency Flux
EZ - Epileptogenic Zone
BCE - Binary Cross-Entropy.

## Appendix A\B\C…, with appendix tile

None.

## References


[1] World Health Organization, "Epilepsy," World Health Organization (WHO) Fact Sheets, 2019. [Online]. Available: https://www.who.int/health-topics/epilepsy. [Accessed: Sep. 23, 2025].
[2] H. Suzuki et al., "Identification of drug-resistant laterality in bilateral temporal lobe epilepsy," Cureus, vol. 17, no. 5, 2025.
[3] W. U. R. Qamar, M.-H. Lee, and B. Abibullaev, "Deep learning in intracranial eeg for seizure detection: advances, challenges, and clinical applications," Front. Neurosci., vol. 19, p. 1677898, 2025.
[4] A. Daida et al., "Ai-based localization of the epileptogenic zone using intracranial eeg," Epilepsia Open, 2025.
[5] J. Cheng et al., "Localization of epileptogenic zone from seeg: Combination of high-frequency energy and synchronous connection in epileptic network analysis," Biomed. Signal Process. Control, vol. 100, p. 107056, 2025.
[6] C. Du et al., "Automated detection of the epileptogenic zone in stereoelectroencephalography for drug-resistant epilepsy using multi-epileptogenic biomarker machine learning," Epilepsy Res., p. 107710, 2025.
[7] ELBehy, A. Hadriche, R. Maalej, and N. Jmail, "Comparison between different source localization and connectivity metrics of spiky and oscillatory meg activities," *Int. J. Electr. Comput. Eng. Syst.*, vol. 15, no. 10, pp. 875–884, 2024.
[8] A. Raghu et al., "Machine learning-based localization of the epileptogenic zone using high-frequency oscillations from seeg: A real-world approach," J. Clin. Neurosci., vol. 135, p. 111177, 2025.
[9] N. Jmail, R. Jarray, A. Hadriche, T. Frikha, and C. Benar, "Separation between spikes and oscillation by stationary wavelet transform implemented on an embedded architecture," *J. Neurol. Sci.*, vol. 381, p. 542, 2017.
[10] A. Aymen, S. E. Khediri, A. Thaljaoui, M. Miladi, and A. Kachouri, "Catalyzing eeg signal analysis: unveiling the potential of machine learning-enabled smart k nearest neighbor outlier detection," Int. J. Inf. Technol., vol. 17, no. 9, pp. 5613–5624, 2025.
[11] Z. Gu, S. Yang, Z. Yu, and F. Liu, "Detection of high-frequency oscillations from intracranial eeg data with switching state space model," in 2024 46th Annu. Int. Conf. IEEE Eng. Med. Biol. Soc. (EMBC), 2024, pp. 1–4.
[12] A. Hadriche, N. Jmail, A. Kachouri, and H. Ghariani, "The detection of evoked potential with variable latency and multiple trial using consensus matching pursuit," in *Proc. 1st Int. Conf. Adv. Technol. Signal Image Process. (ATSIP)*, Sfax, Tunisia, 2014, pp. 316–321.
[13] R. Maalej, A. Hadriche, and N. Jmail, "Artificial intelligence in epilepsy: A narrative review of automated high-frequency oscillation detection and seizure recognition (2022–2025)," *Epilepsy & Seizure*, vol. 18, p. A000175, 2026.
[14] Z. Sadek, A. Hadriche, R. Maalej, and N. Jmail, "Multi-classification of high-frequency oscillations using ieeg signals and deep learning models," *arXiv preprint arXiv:2412.17145*, 2024.
[15] G. Yi, J. Song, W. Zhang, J. Wang, S. Li, and L. Cai, "Cnn with double-side weighted visibility graph for automated classification of high-frequency oscillations in epilepsy," Biomed. Signal Process. Control, vol. 110, p. 108178, 2025.
[16] S. Aslan and H. Bingöl, "Epileptic seizure detection from eeg signals with recurrent neural networks based classification model," J. Phys. Chem. Funct. Mater., vol. 7, no. 2, pp. 14–21, 2024.
[17] Z. Huang et al., "Eeg detection and recognition model for epilepsy based on dual attention mechanism," Sci. Rep., vol. 15, no. 1, p. 9404, 2025.
[18] S. Chaibi and A. Kachouri, "Toward reliable models for distinguishing epileptic high-frequency oscillations (hfos) from non-hfo events using lstm and pre-trained owl-vit vision–language framework," AI, vol. 6, no. 9, p. 230, 2025.
[19] J. Su et al., "A model for epileptic eeg detection and recognition based on multi-attention mechanism and spatiotemporal," Sci. Rep., vol. 15, no. 1, p. 31993, 2025.
[20] V. Adusumilli and M. M. Bee, "Epileptic seizure detection and classification of eeg signal using k-nearest neighbors (knn) compared with anfis-adaptive network-based fuzzy inference system," AIP Conf. Proc., vol. 2816, p. 030001, 2024.
[21] S. Padmakala, "Epileptic seizure detection in rodent IEEG using machine learning: A comparative study of random forest, svm, and gradient boosting models," in 2025 9th Int. Conf. Inventive Syst. Control (ICISC), 2025, pp. 1164–1171.
[22] F. Krikid et al., "Multi-classification of high-frequency oscillations in intracranial eeg signals based on cnn and data augmentation," Signal Image Video Process., vol. 18, no. 2, pp. 1099–1109, 2024.
[23] L. K. Kumari et al., "Advanced epileptic seizure recognition with a hybrid CNN–Bi-LSTM model on eeg signals," in 2025 IEEE 1st Int. Conf. Smart Sustainable Dev. Elect. Eng. (SSDEE), 2025, pp. 1–5.
[24] W. Zhao et al., "Residual and bidirectional lstm for epileptic seizure detection," Front. Comput. Neurosci., vol. 18, p. 1415967, 2024.
[25] T. Fedele et al., "High frequency oscillations detected in the intracranial eeg of epilepsy patients during interictal sleep, patients' electrode location and outcome of epilepsy surgery," CRCNS.org, 2017.
[26] S. Burnos et al., "The morphology of high frequency oscillations (hfo) does not improve delineating the epileptogenic zone," Clin. Neurophysiol., vol. 127, no. 4, pp. 2140–2148, 2016.
[27] S. S. Sikarwar, A. K. Rana, and S. S. Sengar, "Entropy-driven deep learning framework for epilepsy detection using electro encephalogram signals," Neuroscience, vol. 577, pp. 12–24, 2025.

[28] W. Chen et al., "Unsupervised detection of high-frequency oscillations in intracranial electroencephalogram: promoting a valuable automated diagnostic tool for epilepsy," Front. Neurol., vol. 16, p. 1455613, 2025.
[29] S. Lu et al., "Leveraging channel coherence in long-term ieeg data for seizure prediction," IEEE J. Biomed. Health Inform., 2025.
[30] R. Maalej, A. Hadriche, and N. Jmail, "A simulation-based cnn–transformer hybrid model for the classification of high-frequency oscillations in intracranial eeg signals," *Epilepsy & Seizure*, vol. 17, p. A000170, 2025.

## Authors' Profiles



**Rahma Maalej** is a PhD student at the MIRACL Laboratory, University of Sfax, Tunisia. She is affiliated with the Department of STIC at the National School of Electronics and Telecommunications of Sfax (ENET'Com). With three years of experience in higher education, she has already published four research articles in international peer-reviewed journals. Her research focuses on Artificial Intelligence, Data Mining, and Signal Preprocessing, particularly for biomedical applications.



**Abir Hadriche** is an Assistant Professor at the University of Sfax, Tunisia, and a senior researcher within the MIRACL and REGIM laboratories. She holds a PhD in Neurosciences from Aix-Marseille University (France). Her research expertise lies at the intersection of Biomedical Signal Processing and Artificial Intelligence, with a specific focus on modeling brain dynamics and developing automated diagnostic tools for neurological disorders such as epilepsy. She has authored numerous high-impact articles in international journals and serves as a reviewer for several prominent scientific committees in the field of neuroengineering.



**Mohamed Amine Ben Msarra** is a researcher and PhD candidate affiliated with the MIRACL Laboratory at the University of Sfax, Tunisia. Based in the Department of STIC at ENET'Com Sfax, Tunisia, he specializes in Signal Preprocessing and AI-driven diagnostics.



**Nawel Jmail** is an Associate Professor of Signal Processing and a Senior Researcher at the MIRACL Laboratory, University of Sfax, Tunisia. She holds an Engineering degree from National School of Engineers of Sfax, ENIS and a PhD in Neurosciences, conducted in co-tutelle between Aix-Marseille University (France) and the University of Sfax. Having obtained her Habilitation (HDR), she is a leading expert in electrophysiological signal analysis (MEG, EEG, and IEEG). Her research focuses on brain source localization, functional connectivity, and the development of automated biomarkers for epilepsy, including High-frequency Oscillations (HFOs). Dr. Jmail has authored numerous peer-reviewed articles in prestigious journals and maintains strong international collaborations with institutions such as INSERM.

## How to cite this paper:

Rahma Maalej, Abir Hadriche, Mohamed Amine Ben Msarra, Nawel Jmail, "A Feature-Enhanced Hybrid CNN-BiLSTM Framework for Multi-Label Classification of Pathological High-Frequency Oscillations in Intracranial EEG Signals", International Journal of Image, Graphics and Signal Processing(IJIGSP), Vol.18, No.3, pp. 1-16, 2026. DOI:10.5815/ijigsp.2026.03.01